

Tutorials and Examples of UQ/SA in Cardiovascular Modeling

D. Schiavazzi

Department of Applied and Computational Mathematics and Statistics
University of Notre Dame



Jun 28th, 2017
Berkeley-NTNU UQ-SA Workshop
University of California, Berkeley
Berkeley, CA

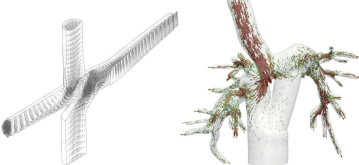
Presentation outline

Three proposed tutorials:

- ✓ I - **OLS and RVM regression** of interface 3D-0D pressure/flow and its use in reduced order modeling.
- ✓ II - Assimilation of heart failure conditions in LPN circulation model **using optimization**.
- ✓ III - Example of **multiresolution spectral expansion** for regression of a non-smooth function.

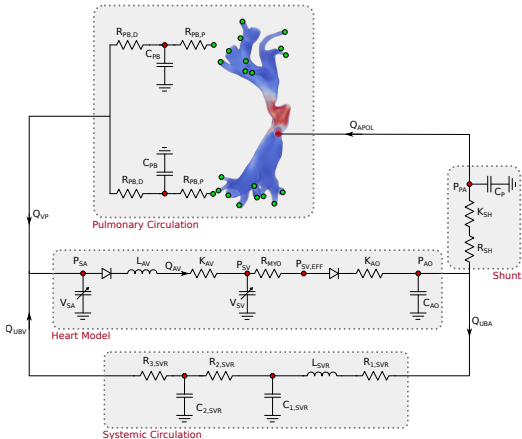
Geometric multi-scale modeling

- ✓ **CFD models** the total cavo-pulmonary connections appeared in the late 90's. Peripheral circulation is marginally accounted.
- ✓ **Modern** approaches:
 - Advanced FE for CFD, **FSI** problems.
 - Implicit **coupling** with circulation network.
 - **Stabilization** at coupled surfaces to prevent backflow divergence.



Dubini et al., 1996

Yang et al., 2012



Multiscale model layout for Single-Ventricle physiology

I - Additional material for the first tutorial

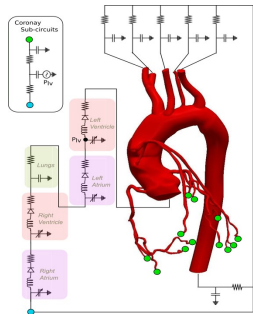
Condensation of multi-scale models

- ✓ **Model tuning**, i.e., selection of boundary conditions to match the physiology of a specific patient is of **paramount importance** in CV Simulation and is affected by multiple error/uncertainty sources.
- ✓ This step is typically performed using **optimization or estimation**, requiring **multiple** model evaluations.
- ✓ These operations become **computationally intractable** for multi-scale models, where a single model solution for a few heart cycles may require **several hours**.
- ✓ We aim to develop an **augmented lumped parameter model** providing similar results to the multi-scale model but requiring a **fraction of a second** to be solved.
- ✓ **Condensation approaches** used in our group:
 - ▶ Optimized **Resistive** surrogate.
 - ▶ Surrogate through **sparse** pressure-flow rate regression.

Resistive surrogate for coronary artery disease

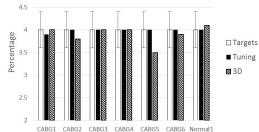
- ✓ Surrogate resistances are **proportional** to the outlet resistances to **preserve the flow split**.
- ✓ The **systemic** surrogate resistances and the **coronary** surrogate resistances are **iteratively refined** until multiscale and surrogate outputs differ less than 10%.

Multiscale layout for coronary simulations

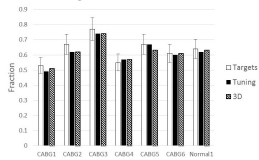


J. S. Tran et al., Computer & Fluids, 2016.

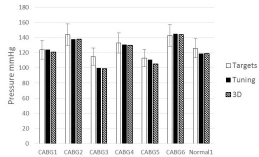
Aorta/coronary flow split



Ejection fraction



Maximum aortic pressure



Regression of 0D-3D interface pressure/flow rate

- ✓ Consider a region $\Omega \subset \mathbb{R}^3$ with boundary $\partial\Omega$ partitioned into **walls** $\Gamma^w = \{\Gamma_j^w, j = 1, \dots, n_w\}$ and **interfaces** $\Gamma = \{\Gamma_j, j = 1, \dots, n\}$.
- ✓ The average **pressure** p_i and **flow rate** q_i at the generic Γ_i are

$$p_i = \frac{1}{|\Gamma_i|} \int_{\Gamma_i} p \, d\Gamma_i, \quad q_i = \int_{\Gamma_i} (\mathbf{v} \cdot \mathbf{n}_i) \, d\Gamma_i$$

- ✓ We assume that the discrete 3D model can be **replaced** by

$$q_i(t) = f(\mathbf{p}, t, \gamma) = \sum_{j=1}^{n_b} \alpha_{j,i}(t, \gamma) \phi_j(\mathbf{p}, t, \gamma), \quad i = 1, \dots, n.$$

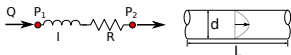
where t represents **time**, $\alpha_i = (\alpha_{1,i}, \dots, \alpha_{n_b,i}) \in \mathbb{R}^{n_b}$ is a vector of **expansion coefficients**, ϕ_j is a set of **generic basis functions**, and γ , a vector of **additional variables**.

- ✓ If we assume **rigid walls** and **negligible inertance** we can neglect dependence from t and γ , this leads to

$$q_i = \sum_{j=1}^{n_b} \alpha_{j,i} \phi_j(\mathbf{p}), \quad i = 1, \dots, n.$$

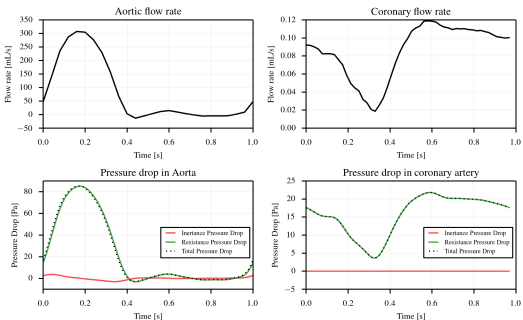
Contribution of inertance

- ✓ Consider the relationship between pressure drop and flow rate in an **idealized rigid cylindrical vessel**.
- ✓ The contribution of inertance and resistance to the overall pressure drop **is separated** for an **aortic** and a **coronary** vessel.



$$\begin{aligned}(p_2 - p_1) &= \Delta p = I \dot{q} + R q \\ &= \left(\frac{\rho L}{\pi r^2} \right) \dot{q} + \left(\frac{8 \nu L}{\pi r^4} \right) q\end{aligned}$$

System	ρ [kg/m ³]	L [m]	ν [Pa·s]
Healthy adult aorta	1.060	0.664	4.0×10^{-3}
Healthy adult coronary	1.060	0.15	4.0×10^{-3}
System	d [m]	I [Pa·s/m ³]	R [Pa·s ² /m ³]
Healthy adult aorta	0.025	1.43×10^{-3}	$2.77 \times 10^{+5}$
Healthy adult coronary	0.0034	1.75×10^{-4}	$1.83 \times 10^{+8}$



OLS Estimator

- ✓ α_i is determined by **minimization of the squared error**:

$$e_i = \sum_{j=1}^m [\mathbf{q}_i - \Phi \boldsymbol{\alpha}_i]_{S_j}^2 = (\mathbf{q}_i - \Phi \boldsymbol{\alpha}_i)^T (\mathbf{q}_i - \Phi \boldsymbol{\alpha}_i).$$

- ✓ The squared error e_i is proportional to the negative log-likelihood of the data for a **linear statistical model of the form**:

$$\mathbf{q}_i = \Phi \boldsymbol{\alpha}_i + \boldsymbol{\epsilon}_i,$$

with **error** $\boldsymbol{\epsilon}_i \sim \mathcal{N}(\mathbf{0}, \sigma^2 I)$, and **likelihood** $\ell_{\boldsymbol{\alpha}_i}(\mathbf{q}_i) = \mathcal{N}(\Phi \boldsymbol{\alpha}_i, \sigma^2 I)$.

- ✓ $\boldsymbol{\alpha}_{i,OLS}$ is **unbiased** and achieves **asymptotic efficiency** with covariance that attains the Cramér-Rao bound.
- ✓ Thus, the **inverse** of the Fisher information matrix at $\boldsymbol{\alpha}_i = \boldsymbol{\alpha}_{i,OLS}$ quantify the **second order statistics** of $\boldsymbol{\alpha}_{i,OLS}$.

$$\mathbf{C}_{\boldsymbol{\alpha}}^{-1} = \mathcal{I} = -\mathbb{E} \left[\frac{\partial^2 \log \ell_{\boldsymbol{\alpha}}(\mathbf{q})}{\partial \boldsymbol{\alpha} \partial \boldsymbol{\alpha}^T} \right] = \frac{1}{\sigma^2} \Phi^T \Phi.$$

RVM Estimator

- ✓ Relevance vector machines combine Bayesian estimation with **sparsity promoting hyper-priors**.
- ✓ Such hyperpriors are specified **over each coefficient** α_i as independent, zero-mean, Gaussians with precisions $\beta = (\beta_1, \beta_2, \dots, \beta_{n_b})$:

$$P(\alpha_i | \beta) = \frac{1}{(2\pi)^{n_b/2} \prod_{k=1}^{n_b} \beta_k} \exp \left[-\frac{1}{2} \alpha_i^T \mathbf{Z} \alpha_i \right]$$

with \mathbf{Z} being a diagonal matrix with $Z_{j,j} = \beta_j$.

- ✓ The posterior $P(\alpha_i | \mathbf{q}_i, \beta, \sigma^2) \sim \mathcal{N}(\mu, \Sigma)$ **is also Gaussian** with

$$\mu = \sigma^{-2} \Sigma \Phi \mathbf{q}_i, \quad \Sigma = (\mathbf{Z} + \sigma^{-2} \Phi^T \Phi)^{-1}$$

- ✓ Values of β_j are determined by **iterative maximization of the marginal log-likelihood**

$$\mathcal{M}(\beta) = \log P(\mathbf{q}_i | \beta, \sigma^2) = -\frac{1}{2} \left[N \log(2\pi) + \log |\mathbf{C}| + \mathbf{q}_i^T \mathbf{C}^{-1} \mathbf{q}_i \right],$$

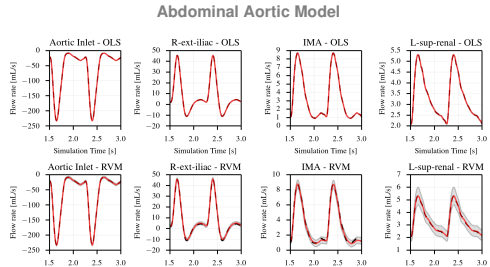
with $\mathbf{C} = \sigma^2 \mathbf{I} + \Phi \mathbf{Z}^{-1} \Phi^T$.

Regression results for aortic and coronary model

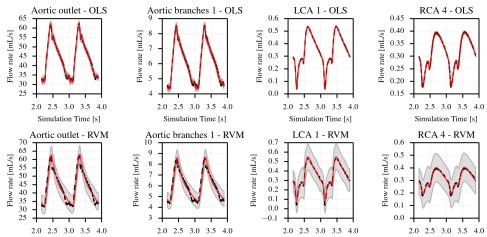
Abdominal Aorta Model - Open loop BC



Coronary Model - Closed loop BC

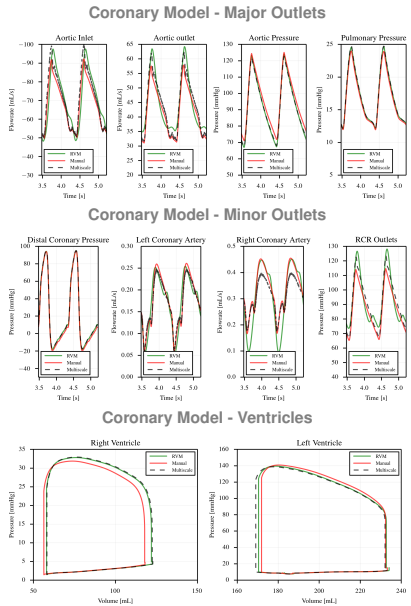
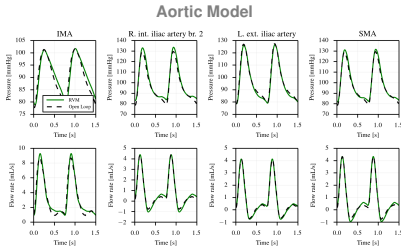


Coronary Circulation Model



Inclusion in closed loop circulation models

- ✓ We **integrate** the regressor in the respective 0D network models.
- ✓ OLS regressors are **not stable and lead to divergence of RK4 iterations.**
- ✓ RMV regressors **are stable** and lead to LPN results that closely approximate the multiscale results.
- ✓ RMV results are compared to **optimally tuned** equivalent resistors surrogates.

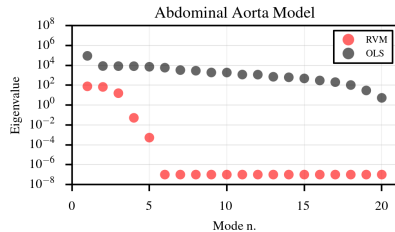
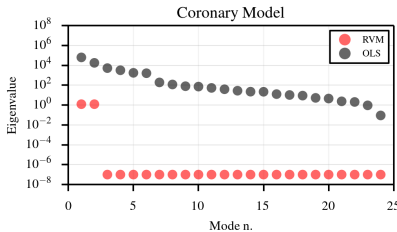


Amplification of pressure perturbations

- ✓ Stability considers how outlet flow rates are **amplified** by the surrogate as a result of pressure perturbations.
- ✓ Consider a **Gaussian pressure noise of uniform variance** σ^2 and flow rates at the interface written as a linear combination of outlet pressures:

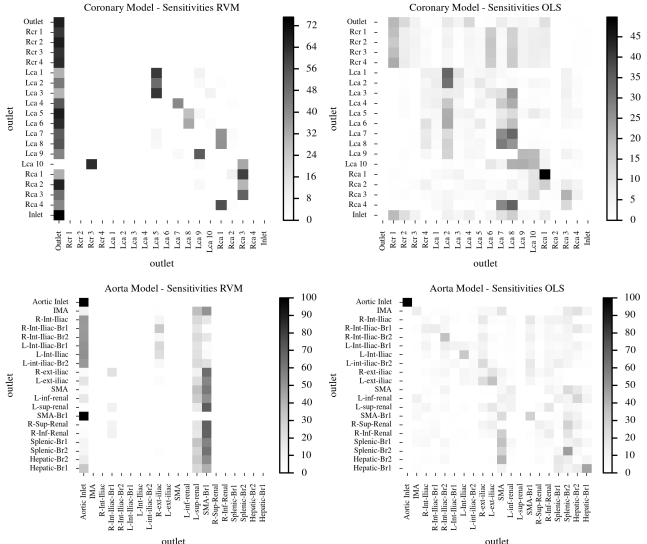
$$q_i = \sum_{j=2}^{n+1} \alpha_{j,i} p_j = \hat{\alpha}_i \mathbf{p}, \text{ and } \mathbf{q} = \mathbf{A} \mathbf{p}$$

- ✓ A **pressure perturbation** $\delta \mathbf{p} \sim \mathcal{N}(\mathbf{0}, \sigma^2 \mathbf{I})$ will generate a **flow rate perturbation** $\delta \mathbf{q} \sim \mathcal{N}(\mathbf{0}, \sigma^2 \mathbf{A} \mathbf{A}^T)$.
- ✓ The eigenvalues of $\mathbf{A} \mathbf{A}^T$ thus represent the **noise amplification factors** through the linear transformation \mathbf{A} .



Direct sensitivities of interface flow rates

- Entries in each row **have sum equal to 100%** and quantify the effect of the outlet listed in the corresponding column.



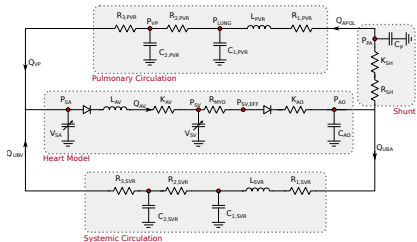
II - Additional material for the second tutorial

Data assimilation for lumped parameter circulation models

- ✓ Once a surrogate model is available the parameter estimation problem can be solved using a **lightweight lumped parameter model** that solves in **a fraction of a second**.
- ✓ **Features** of the lumped parameter models we consider:
 - ▶ **Non-linearity** due to heart contraction, unidirectional valves, non linear resistors (e.g., BT shunt).
 - ▶ **Only time statistics** are available for clinical measurements. For example, maximum/average/minimum pressure/velocity/volume.
- ✓ Optimization provides **only point estimates** for the model parameters and cannot handle target uncertainty.
- ✓ Filtering approaches can handle non linear models (e.g., extended/ensemble Kalman filters) but **require full time histories** for the measurements of interest (rarely available).
- ✓ We therefore use **adaptive MCMC** to sample from the joint posterior distribution of parameters.
- ✓ All good, but ... **are the parameters Identifiable?**

Parameter Estimation in Norwood circulation models

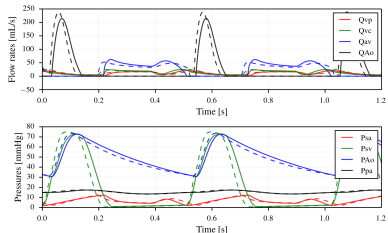
Norwood Circulation Model



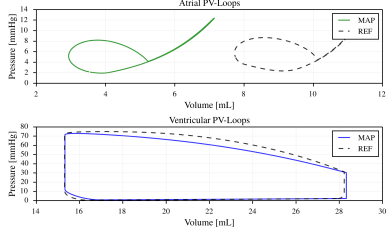
Clinical target matching

Target Quantity	Model Results	Target AV	Target SD	Weight
$P_{ao,av}$	49.568	48.855	2.442	0.5
$P_{ao,min}$	30.610	31.449	1.572	1.0
$P_{ao,max}$	72.625	73.625	3.681	1.0
$P_{sa,av}$	6.484	6.503	0.325	1.0
$P_{sv,max}$	72.972	74.933	3.746	1.0
$V_{sv,max}$	28.328	28.230	1.411	1.0
Q_p/Q_s	0.811	0.831	0.041	1.0
$P_{pa,av}$	15.034	15.126	0.756	1.0
CO	25.495	25.337	1.266	0.5
$Q_{VC,S}$	25.104	24.683	1.234	8.0
$Q_{VC,M}$	4.873	4.853	0.242	8.0
$Q_{VC,D}$	23.811	24.514	1.225	8.0
$Q_{VC,A}$	5.435	5.437	0.271	8.0
$Q_{PV,S}$	21.178	19.633	0.981	12.0
$Q_{PV,M}$	0.239	0.240	0.012	12.0
$Q_{PV,D}$	16.604	16.094	0.804	12.0
$Q_{PV,A}$	7.189	7.113	0.355	12.0
$P_{pa,min}$	13.376	13.405	0.670	1.0
$P_{pa,max}$	17.264	17.239	0.861	1.0
$P_{sv,0}$	2.280	2.251	0.830	1.0
$P_{sa,max}$	12.372	12.228	0.559	1.0

MAP Flow rates and Pressures

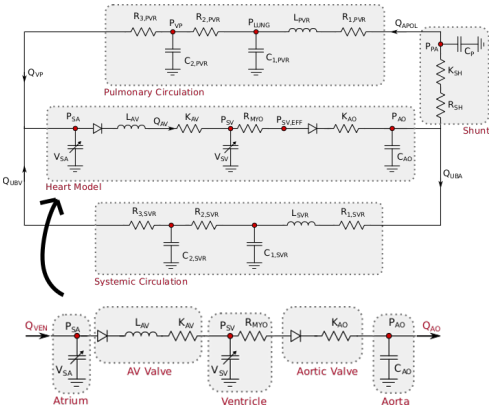


MAP Atrial and ventricular PV-loops



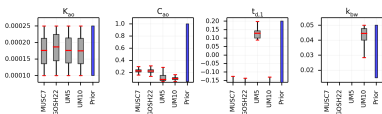
Multi-level Bayesian estimation of Heart model parameters

- ✓ Heart model contains **most** of the parameters and non linearities.
- ✓ Prescribed venous and aortic flow are **measured** through echo-Doppler/PC-MRI.
- ✓ **Multi-level estimation:** we **preliminary determine** the posteriors of the heart model parameters and **use this as prior** for full model parameter estimation.



MAP patient physiology and parameter learning

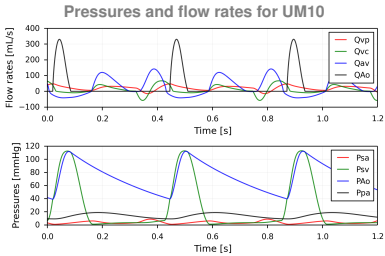
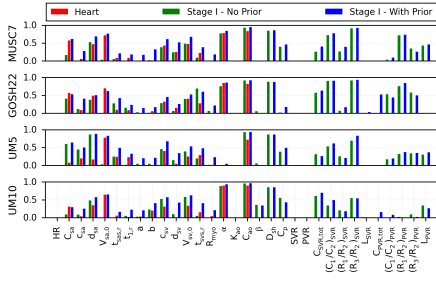
Additional parameter distributions - Norwood Model



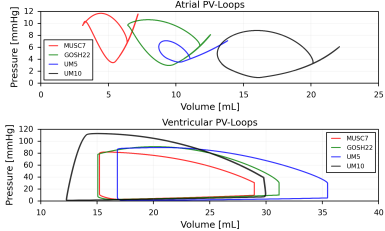
✓ Parameter learning factor estimated as:

$$\theta = 1 - \sqrt{\frac{V[\mathbf{y}|\mathbf{d}]}{V[\mathbf{y}]}}$$

Parameter Learning factors



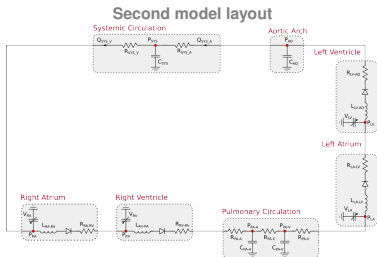
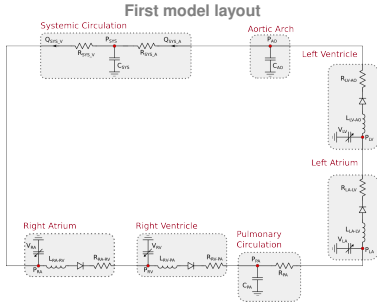
Atrial and Ventricular PV-loop for UM10



D. E. Schiavazzi et al., IJNMBE, 2016.

Estimating pulmonary pressures in diastolic heart failure

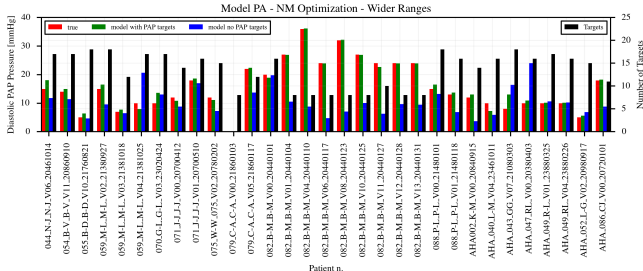
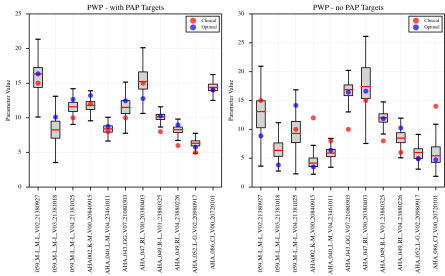
- ✓ Group II PH: **elevated pulmonary pressure from left heart dysfunction.**
- ✓ This type of dysfunction (left ventricular diastolic dysfunction) is **more difficult to diagnose** since it is not associated with a drop in ejection fraction and cardiac output.
- ✓ **Early diagnosis** of group II PH from minimally invasive clinical or sensor data, will help **preventing the occurrence and reduce the mortality** associated with this disease.
- ✓ Can integration of **physics-based modeling and lumped parameter circulation systems** and non-invasive data collection **improve the prediction of pulmonary pressures** (systolic, diastolic and wedge pressures) that are difficult to measure non-invasively.



PAP errors in single visit prediction

- ✓ **Anonymized clinical targets** were obtained for several patients from a Google ATAP collaboration.
- ✓ Using Nelder-Mead optimization and adaptive MCMC estimation, the **diastolic, systolic and wedge pulmonary pressures where blindly estimated** for all visits and correlated with the total number of available targets.

Distributions of predicted PWP in heart failure patient

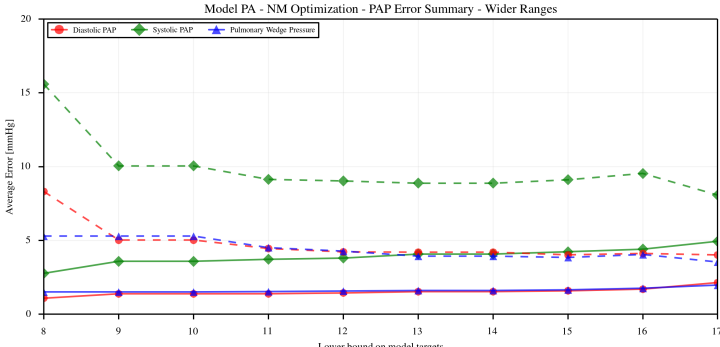


PAP errors in single visit prediction - MCMC

- ✓ MCMC estimation on the patients with more than 11 REDCap entries leads to improved average errors of about **7 mmHg for Systolic PAP**, **5 mmHg for Diastolic PAP** and **3 mmHg for PWP**.

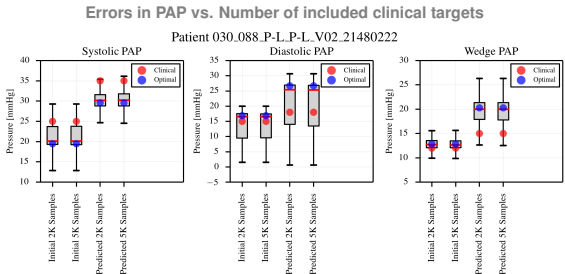
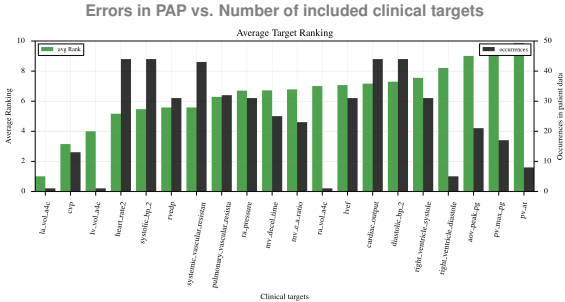
REDCap Token	Units	Std	REDCap Token	Units	Std
heart_rate2	[mmHg]	3.0	mv_e_a_ratio	-	0.2
systolic_bp_2	[mmHg]	1.5	pv_at	[ms]	6.0
diastolic_bp_2	[mmHg]	1.5	pv_max_pg	[mmHg]	0.5
cardiac_output	[L/min]	0.2	ra_pressure	[mmHg]	0.5
systemic_vascular_resistan	[CGS]	50.0	ra_vol_a4c	[mL]	3.0
pulmonary_vascular_resista	[CGS]	5.0	la_vol_a4c	[mL]	3.0
cvp	[mmHg]	0.5	lv_esv	[mL]	10.0
right_ventricle_diastole	[mmHg]	1.0	lv_vol_a4c	[mL]	20.0
right_ventricle_systole	[mmHg]	1.0	lvef	-	2.0
rvedp	[mmHg]	1.0	pap_diastolic	[mmHg]	1.0
aov_mean_pg	[mmHg]	0.5	pap_systolic	[mmHg]	1.0
aov_peak_pg	[mmHg]	0.5	wedge_pressure	[mmHg]	1.0
mv_decel_time	[ms]	6.0			

PAP errors vs. Number of included clinical targets



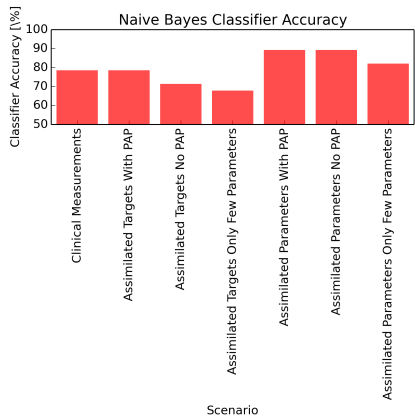
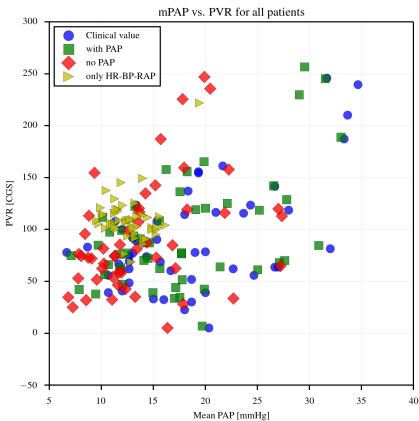
Follow-up visit prediction using Bayesian update

- ✓ Prediction of PAP follow-up trends using Bayesian update is successful in **46%** of the cases for **systolic** pulmonary pressure (24 patients), **58%** for **diastolic** pulmonary pressure (24 patients) and **80%** for **wedge** pulmonary pressure (10 patients).



Heart Failure Detection

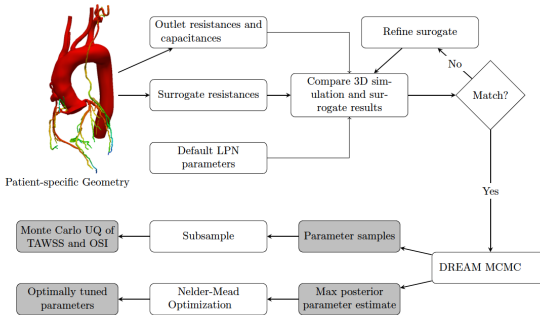
- ✓ Patients with pulmonary hypertension **were identified** in the cohort of 84 patients based on **mPAP vs. PVR**. The same quantities were predicted through models from a **smaller number of available targets** (with PAP, No PAP, only HR-BP-RAP).
- ✓ A **Naive Bayes classifier** is used to identify cases of pulmonary hypertension. Classification using assimilated parameters **gives good accuracy even if the the pulmonary pressures are not included**.



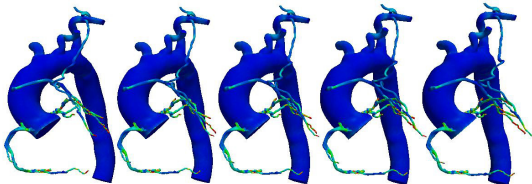
III - Additional material for the third tutorial

Data Assimilation and MCS in coronary artery disease

Workflow for UQ in coronary artery disease

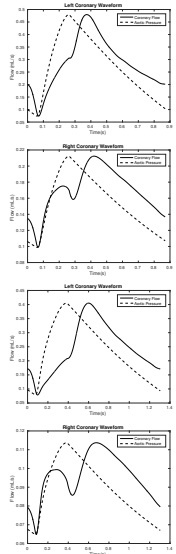


MCS convergence of TAWSS Standard Deviation (10 - 20 - 30 - 40 - 50 samples)



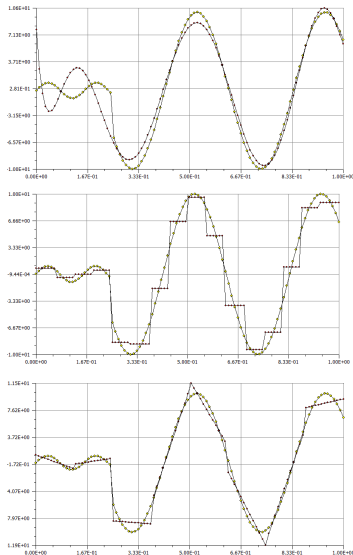
J. S. Tran et al., Computer & Fluids, 2016.

Coronary flow waveforms



Why Alpert Multiwavelets?

- ✓ Multiresolution basis built on top of the **Legendre Polynomials**.
- ✓ It is still an **orthonormal** basis.
- ✓ Coefficients: **statistics** and feature **detection**.
- ✓ **Generalize** Wiener-Legendre and Wiener-Haar basis expansions.
- ✓ Has the ability to represent **discontinuous** responses.
- ✓ Piecewise smooth responses are **sparse** in the Alpert basis and coefficients are typically organized in compact subtrees.
- ✓ For **non-uniform random inputs**, however, the number of samples **may increase by transforming** the random inputs.



Alpert, 1993, Le Maître et al., 2004, Tryoen et al., 2012

Multiscaling orthogonality to arbitrary PDFs

- ✓ Probability space (Ω, \mathcal{F}, P) and random variable $y : \Omega \rightarrow \Sigma_y$.
- ✓ Input probability measure $\rho^k(y^{(j)})$, $j = 1, \dots, n_q$ defined on the k -th partition $\Sigma_y^k \subset \Sigma_y$, **sampled at quadrature points**.
- ✓ Multiscaling family $\{\phi_i, i = 0, \dots, m - 1\}$ built **using the three-term recurrence**:

$$\phi_{-1} = 0, \phi_0 = 1, \phi_{i+1}(y) = (y - \alpha_i) \phi_i(y) - \beta_i \phi_{i-1}. \quad i = 0, \dots, m - 1,$$

where:

$$\alpha_i = \frac{\langle \phi_i, y \phi_i \rangle_{\mathcal{H}^k}}{\langle \phi_i, \phi_i \rangle_{\mathcal{H}^k}}, \text{ and } \beta_i = \frac{\langle \phi_i, \phi_i \rangle_{\mathcal{H}^k}}{\langle \phi_{i-1}, \phi_{i-1} \rangle_{\mathcal{H}^k}}.$$

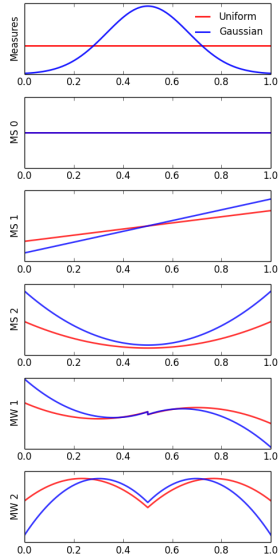
- ✓ Every inner product is evaluated using **numerical quadrature**:

$$\langle f, g \rangle_{\mathcal{H}^k} = \int_{\Sigma_y^k} f(y) g(y) \rho^k(y) dy \approx \sum_{j=1}^{n_q} f(y^{(j)}) g(y^{(j)}) \rho^k(y^{(j)}) w_j,$$

where w_j denotes the weights for the selected quadrature rule (**double** Clenshaw-Curtis quadrature in this study).

Construction of orthogonal multiwavelets

- ✓ $\mathbf{V}_{m,0}^k$ is the space of polynomials with order less than m in $[0, 1]$, spanned by $\{\phi_i, i = 0, \dots, m - 1\}$.
- ✓ Construct a basis $\{\psi_i, i = 0, \dots, m - 1\}$ for $\mathbf{W}_{m,0}^k$ that **complements** $\mathbf{V}_{m,0}^k$ to the space of continuous polynomials of order less than m defined **separately on $[0, 1/2]$ and $[1/2, 1]$** , i.e., $\mathbf{W}_{m,0}^k \perp \mathbf{V}_{m,0}^k$, and $\mathbf{V}_{m,0}^k \oplus \mathbf{W}_{m,0}^k = \mathbf{V}_{m,1}^k$:
 1. **Build** $2m$ functions which span the space of polynomials of degree less than m on the interval $[-1, 0)$ and on $[0, 1]$.
 2. **Orthogonalize** m of them, first to $\{1, y, y^2, \dots, y^{m-1}\}$, then to $\{y^m, y^{m+1}, \dots, y^{2m-1}\}$.
 3. Implement **orthogonality** between ψ_i and ψ_j for $i \neq j$.
 4. **Rescale** to $[0, 1]$ and **normalize** to have $\langle \psi_i, \psi_j \rangle_{\mathcal{H}^k} = \delta_{i,j}$.



Alpert B. K., SIAM JMA, 1993.

Multi-resolution ANOVA for adaptivity

- ✓ Consider a **model** $u(y) : [0, 1] \rightarrow \mathbb{R}$, whose response is **approximated** using:

$$u(y) \approx \sum_{i=0}^{m-1} [\alpha_i \phi_i(y) + \beta_i \psi_i(y)].$$

- ✓ As all $\{\phi_i(y), \psi_i(y), i = 0, \dots, m-1\}$ except $\phi_0(y)$ have **zero average** over $[0,1]$, the variance $\mathbb{V}[u(y)]$ can be decomposed as follows:

$$\mathbb{V}[u(y)] \approx \sum_{i=1}^{m-1} \alpha_i^2 + \sum_{i=1}^{m-1} \beta_i^2 = \mathbb{V}_{MS} + \mathbb{V}_{MW}$$

where the multiscaling and multiwavelet variances are identified. We use the relative importance of \mathbb{V}_{MW} and \mathbb{V}_{MS} to **determine whether we need to refine** $[0, 1]$ into $[0, 1/2)$ and $[1/2, 1]$.

Monolithic approach in multiple dimensions

- ✓ For $d > 1$, **multi-index** $\mathbf{i} \in \mathcal{I} = \{(i_1, \dots, i_d) : 0 \leq i_l < m_l, l = 1, \dots, d\}$

$$\phi_{\mathbf{i}}(\mathbf{y}) = \phi_{i_1}(y_1) \dots \phi_{i_d}(y_d), \quad \mathcal{S}_0^{\mathbf{m}} = \{\phi_{\mathbf{i}}(\mathbf{y}) : \mathbf{i} \in \mathcal{I}\}.$$

- ✓ **Permutations:** $\mathbf{q} \in \mathcal{Q} = \{(q_1, \dots, q_d) : q_l \in \{0, 1\}, l = 1, \dots, d\}$.

$$\psi_i^0 = \phi_i, \quad \psi_i^1 = \varphi_i, \quad \psi_{\mathbf{i}}^{\mathbf{q}}(\mathbf{y}) = \psi_{i_1}^{q_1}(y_1) \dots \psi_{i_d}^{q_d}(y_d),$$

- ✓ The **orthogonal basis** set at $j = 0$ is

$$\mathcal{W}_0^{\mathbf{m}} = \{\psi_{\mathbf{i}}^{\mathbf{q}}(\mathbf{y}) : \mathbf{i} \in \mathcal{I}, \mathbf{q} \in \mathcal{Q} \setminus \{0\}\},$$

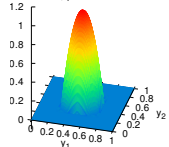
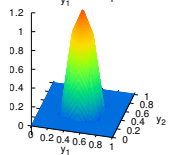
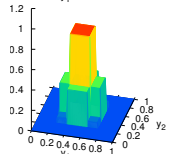
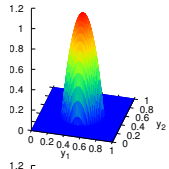
- ✓ At **higher resolutions**, $\mathbf{k} \in \mathcal{K} = \{(k_1, \dots, k_d) : 0 \leq k_l \leq 2^j - 1, l = 1, \dots, d\}$

$$\psi_{j,\mathbf{i},\mathbf{k}}^{\mathbf{q}}(\mathbf{y}) = 2^{jd/2} \psi_{i_1}^{q_1}(2^j y_1 - k_1) \dots \psi_{i_d}^{q_d}(2^j y_d - k_d)$$

- ✓ **Expansion:** given $\mathbf{m} = (m_1, \dots, m_d)$

$$u(\mathbf{y}) = \sum_{\mathbf{i} \in \mathcal{I}} \alpha_{0,\mathbf{i},0} \psi_{0,\mathbf{i},0}^0(\mathbf{y}) + \sum_{j=0}^{\infty} \sum_{\mathbf{k} \in \mathcal{K}} \sum_{\mathbf{q} \in \mathcal{Q}} \sum_{\mathbf{i} \in \mathcal{I}} \alpha_{j,\mathbf{i},\mathbf{k}} \psi_{j,\mathbf{i},\mathbf{k}}^{\mathbf{q}}(\mathbf{y})$$

$$u(\mathbf{y}) = \sum_{i=1}^{\infty} \alpha_i \psi_i(\mathbf{y})$$



Binary Refinements and Multivariate Complexity

Monolithic multivariate expansion:

$$u(\mathbf{y}) = \sum_{\mathbf{i} \in \mathcal{I}} \alpha_{0,\mathbf{i},0} \psi_{0,\mathbf{i},0}^0(\mathbf{y}) + \sum_{j=0}^{\infty} \sum_{\mathbf{k} \in \mathcal{K}} \sum_{\mathbf{q} \in \mathcal{Q}} \sum_{\mathbf{i} \in \mathcal{I}} \alpha_{j,\mathbf{i},\mathbf{k}} \psi_{j,\mathbf{i},\mathbf{k}}^{\mathbf{q}}(\mathbf{y})$$

✓ **Multi-element** approach:

- ✓ Enables **parallel regression** on separate parameter space partitions.
- ✓ **No refinement** needed at lower resolutions, but new elements.

✓ The hypercube partitions are stored using a **binary tree**:

- ✓ Avoids need for **full tensor product** of multiwavelets basis (adaptive selection of interaction terms becomes possible).
- ✓ Multiwavelet basis **do not need to be mixed up** along different axis.

Dependent inputs - change of measure

- ✓ In practical applications, random inputs are **often not independent**, e.g., M samples $\mathbf{y}^{(k)}$, $k = 1, \dots, M$ generated from the joint distribution $\rho(\mathbf{y})$ **through MCMC**.
- ✓ Consider a **truncated multiwavelet expansion** of the stochastic response $u(\mathbf{y})$:

$$u(\mathbf{y}) \approx \sum_{\mathbf{i}=1}^P \alpha_{\mathbf{i}} \psi_{\mathbf{i}}(\mathbf{y})$$

with a multi-index order $\mathbf{i} = (i_1, i_2, \dots, i_d)$, $\mathbf{i} : \mathbb{N}_{\geq 0} \rightarrow \mathbb{N}_{\geq 0}^d$.

- ✓ The family $\psi_{\mathbf{i}}(\mathbf{y})$ is orthogonal to the measure $\prod_{i=1}^d \rho_i(y_i) \neq \rho(\mathbf{y})$, i.e., the **product of the marginals**.
- ✓ The **moments** of $u(\mathbf{y})$ with order p are

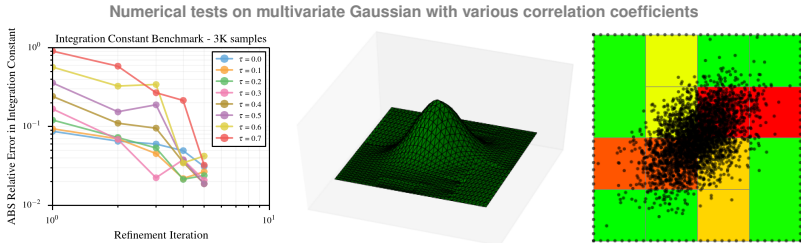
$$\nu^p = \int_{\Omega} [u(\mathbf{y})]^p \rho(\mathbf{y}) d\mathbf{y}.$$

Dependent inputs from MCMC

- ✓ By **multiplying and dividing** by the product of the marginals $\prod_{i=1}^d \rho_i(y_i)$ and *changing the measure*, we obtain:

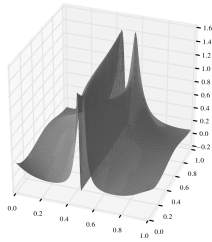
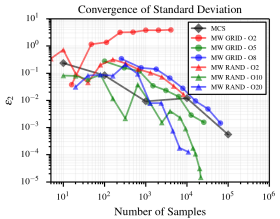
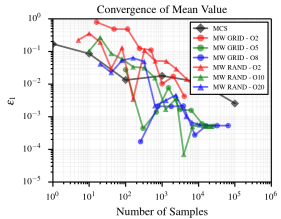
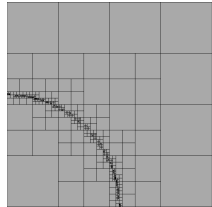
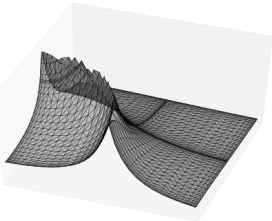
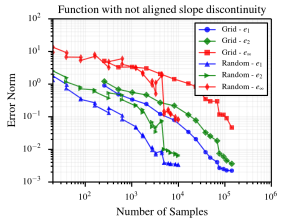
$$\nu_p = \int_{\Omega} \left[u(\mathbf{y})^p \frac{\rho(\mathbf{y})}{\prod_{i=1}^d \rho_i(y_i)} \right] \prod_{i=1}^d \rho_i(y_i) d\mathbf{y} = \int_{\Omega} f(\mathbf{y}) \prod_{i=1}^d \rho_i(y_i) d\mathbf{y}.$$

- ✓ Note also that regression of $f(\mathbf{y})$ from $\{u(\mathbf{y}^{(i)}) : i = 1, \dots, M\}$ **requires the computation** of $\{\beta^{(k)} = \rho(\mathbf{y}^{(k)}) / \prod_{i=1}^d \rho_i(y_i^{(k)})\}, k = 1, \dots, M\}$.

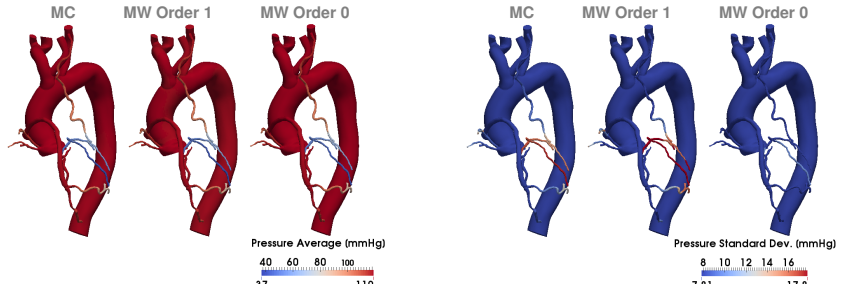


Soize and Ghanem, SIAM JSC, 2004.

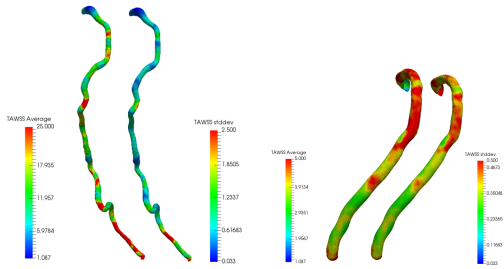
Validation on benchmark problems



Validation on CV simulation



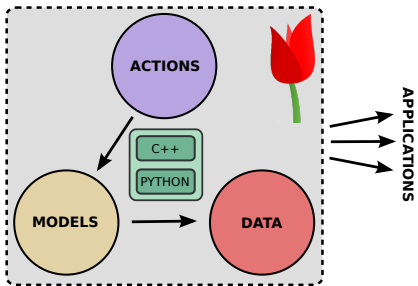
Applications to coronary artery disease (sub-models)



IV - Software: tulip and SimVascular



tulip: a software library for sensor data assimilation and uncertainty analysis of computer models in physiology



```
# Import UQ Library
import tulipUQ as uq
# Import Computational Model Library
import tulipCM as cm
# Import Data Library
import tulipDA as da
# Import Action Library
import tulipAC as ac

# Set Data Object
data = da.daData_multiple_Table()
data.readFromFile('data/dataFile.txt')

# Create Model
model = cm.cmModel()

# Assign Data Object To Model
model.setData(data)

# Set Action
action = ac.acAction(params)

# Set Model in Action
action.setModel(model)

# Compute
action.go()
```



NSF Funded Initiative:

PI - Alison Marsden, Ph.D.
Stanford University

PI - Shawn Shadden
UC Berkeley

PI - Nathan Wilson
OSMSC

Features:

- ✓ Complete **opensource** pipeline from image data to simulation results.
- ✓ Combined 2D and 3D **segmentation** tools.
- ✓ Solid modeling **boolean** operations.
- ✓ **Meshing** tools with adaptation.
- ✓ Readily available **physiological** boundary conditions (resistances, RCR, coronary).
- ✓ **Multiscale** modeling capabilities.
- ✓ Extensive online tutorial and **help** system.



Visit us at:

<http://simvascular.github.io/>

Acknowledgements

Students/Postdocs:

- ✓ Xue Li (ND)
- ✓ Casey M. Fleeter (Stanford)
- ✓ Justin S. Tran (Stanford)

Collaborators:

- ✓ Alison L. Marsden, Ph.D.
- ✓ Gianluca Iaccarino, Ph.D.
- ✓ John K. Eaton, Ph.D.
- ✓ Alireza Doostan, Ph.D.
- ✓ Filippo Coletti, Ph.D.

Clinicians:

- ✓ Jeffrey Feinstein, M.D., M.P.H.
- ✓ Andrew M. Kahn, M.D., Ph.D.
- ✓ Tain-Yen Hsia, M.D., M.Sc.

More Info at:

www.nd.edu/~dschiava

Software:

- ✓ Simvascular (simvascular.github.io)
- ✓ Simtk.org portal

